*Supplementary Methods:*

**Metabric cohort analysis.** The Metabric breast cancer dataset was preprocessed, summarized and quantile-normalized from the raw expression files generated by Illumina BeadStudio (R packages: beadarray v2.4.2 and illuminaHuman v3.db_1.12.2). Raw Metabric files were downloaded from European genome-phenome archive (EGA) (Study ID: EGAS00000000083). Data files of one Metabric sample were not available at the time of our analysis, and were therefore excluded. The most variable probe for RIOK3 was treated as the representative of RIOK3 abundance levels. $Log_2$ scaled data was used for differential mRNA abundance analysis between PAM50 subtypes. Metabric analysis and visualisations were prepared in R statistical environment (v3.0.1). Cox proportional hazards model was used to estimate the hazard ratio, and Wald test was used to test the significance of outcome difference between the low- and high-RIOK3 expression groups.

**Additional qPCR primers.** CA9 F CTTGGAAGAAATCGCTGAGG, CA9 R TGGAAGTAGCGGCTGAAGTC, ADM F GCCTGCCCAGACCCTTAT, ADM R GTAGCGCTTGACTCGGATG, SERPINE1 F AAGGCACCTCTGAGAACTTCA, SERPINE1 R CCCAGGACTAGGCAGGTG.

**Additional cell lines.** SK-OV-3 and MCF7 were obtained from European Collection of Cell Cultures (Salisbury, UK) and maintained in DMEM + 10% FBS. U87-MG and HCT 116 were obtained from Cancer Research UK cell services (Clare Hall, South

Mimms, UK). U87-MG was maintained in DMEM + 10% FBS. HCT 116 was maintained in McCoy's 5A + 10% FBS.

**Inducible shRNA vectors.** pTRIPZ plasmid targeting RIOK3 (shRIOK3; V2THS_238966) or non-silencing (shNS; RHS4743) was acquired from Thermo Scientific. Lentivirus packaging, titration and transduction was carried out as detailed in materials and methods. shRNA was induced with 1 µg/mL doxycycline 48 h prior to and during experiments.

**DMOG treatment.** Dimethyloxalylglycine (DMOG, Sigma-Aldrich) was dissolved in PBS to 150 mM and stored at -80°C. Samples were exposed to 0.5 mM DMOG for 24 h before cell lysis for immunoblot analysis.

**RIOK3 expression vectors.** pDONR223-RIOK3 plasmid was acquired from Addgene (Plasmid 23537). RIOK3 cDNA was PCR amplified using GAATTCCCATGGATCTGGTAGGAGTG (NcoI For) for cloning into pENTR4 no ccDB (686-1) (Addgene plasmid 17424) or GAATTCGTCGACCTGGTAGGAGTGGCATCG (SalI For) for cloning into pENTR4-GFP-C1 (w392-1) (Addgene plasmid 17396) or GAATTCGTCGACCTGGTAGGAGTGGCATCG (SalI For) for cloning into pENTR4-FLAG (w210-2) (Addgene plasmid 17423) and a common reverse primer GAATTCTCTAGACTATTCATCATATAGTAG (XbaI Rev). PCR products were digested with the indicated restriction enzymes (NEB, Hertfordshire, UK), separated by agarose gel electrophoresis, gel extracted and ligated into the indicated digested

pENTR vector. Ligated plasmids were transformed into TOP10F' cells (Life Technologies). All plasmids were sequence verified using pENTR primers (For GGATAACCGTATTACCGCTAG, Rev GTAACATCAGAGATTTTGAGACAC). The cDNA were then cloned into pLenti CMV Puro DEST (w118-1) (Addgene plasmid 17452) using LR clonase kit (Life Technologies) and transformed into STBL3 cells. Lentivirus packaging was carried as described in materials and methods with a modification to use the following plasmids pMDLg/pRRE (Addgene plasmid 12251), pRSV-Rev (Addgene plasmid 12253) and pMD2.G.

**Timelapse video.** MDA-MB-231 were seeded in 24-well ImageLock Plates (Essen BioScience, Hertfordshire, UK) and allowed to attach overnight. Cell migration was monitored on an Incucyte EX (Essen BioScience) with images captured every 5 min. Images in a series were opened using ImageJ, converted to stacks, sorted on label, cropped and then saved as .AVI video files.

**Cell proliferation assay.** MDA-MB-231 cells were seeded at 500 cells/well in black 96-well plates and allowed to attach overnight. Measurements of cell density were made using CyQuant (Life Technologies) on day 1, 3, 5 and 7 using a SpectraMax M2e platereader (Molecular Devices; Sunnyvale, CA).

**Site directed mutagenesis.** pENTR RIOK3 mutants were generated using the GeneArt® Site-Directed Mutagenesis System (Life Technologies) following the manufacturers protocol. RIOK3 M359G mutant was generated using the following primers F AAACACATTTTAGTTGGGTCTTTTATTGGCCA, R

TGGCCAATAAAAGACCCAACTAAAATGTGTTT. RIOK3 I422A mutant was generated using the following primers F GGAAAGGTCTGGTTGGCCGATGTCAGTCAGTC, R GACTGACTGACATCGGCCAACCAGACCTTTCC. Both plasmids were sequence verified, as above. Mutant RIOK3 cDNA was LR cloned into pLenti CMV Neo DEST (705-1) (Addgene plasmid 17392), packaged into lentivirus and transduced into HEK-293 cells, as detailed above.

**Analogue sensitive kinase assay.** Analogue sensitive kinase assay was conducted as described.[1] $N^6$-Benzyladenosine-5'-O-(3- thiotriphosphate) was acquired from BIOLOG Life Science Institute (Bremen, Germany) and p-nitrobenzylmesylate from Abcam (Cambridge, UK).

**Fluorescence recovery after photobleaching (FRAP).** FRAP was carried out on GFP-RIOK3-expressing MDA-MB-231 cells grown in glass bottom dishes (MatTek Corporation, Ashland, MA). Serial images were captured on a Zeiss 510 Inverted Confocal microscope using 63× objective lense.

**References**

1 Koch A, Hauf S (2010). Strategies for the identification of kinase substrates using analog-sensitive kinases. *Eur J Cell Biol* **89:** 184-193.

2 Curtis C, Shah SP, Chin SF, Turashvili G, Rueda OM, Dunning MJ *et al* (2012). The genomic and transcriptomic architecture of 2,000 breast tumours reveals novel subgroups. *Nature* **486:** 346-352.

*Supplementary Figure Legends:*

Figure S1: Expression of RIOK3 in the Metabric cohort.[2] Breast cancer subtypes were classified either by hormonal receptor status (ER-/PgR-/HER2-, HER2-, HER2+, ER-, ER+) or by PAM50 (Basal, Her2, LumB, LumA, Normal-like). (A) Box-whisker plots of RIOK3 expression showing median, upper and lower quartiles and 95% range of mRNA abundance levels. (B) Comparison of mRNA abundance levels for the PAM50 subtypes was carried out using ANOVA followed by Tukey's post-hoc test. diff = $\log_2$ fold change, lwr = lower 95% confidence interval, upr = upper 95% confidence interval. (C) Spearman correlation between RIOK3 expression and hypoxia signature in the basal subgroup (n = 331). (D) Kaplan-Meier analysis of the Metabric cohort demonstrating poorer overall survival (10 year truncated) for breast cancer patients with relatively higher expression of RIOK3. Patients were dichotomized by median into 50% low- and 50% high-RIOK3 expression groups based on mRNA expression.

Figure S2: Expression of CA9, ADM and SERPINE1 are increased in MDA-MB-231 cells during hypoxia in a HIF dependent manner. Expression of CA9 (A), ADM (B) and SERPINE1 (C) mRNA is increased in MDA-MB-231 cells during exposure to 0.1% $O_2$ (mean $\pm$ SEM, n = 3). (D) Up-regulation of CA9 mRNA in MDA-MB-231 cells is suppressed following transfection with siRNA targeting HIF1$\alpha$ or HIF1$\alpha$ and HIF2$\alpha$ (mean $\pm$ SEM, n = 4, repeated measures one-way ANOVA). Up-regulation of ADM (E) and SERPINE1 (F) mRNA in MDA-MB-231 cells is suppressed following

transfection with siRNA targeting HIF2α or HIF1α and HIF2α (mean ± SEM, n = 4, repeated measures one-way ANOVA).

Figure S3: Expression of RIOK3 protein is increased in MCF7 (A), HCT 116 (B) and U-87 MG (C) cells during exposure to hypoxia. (D) Expression of RIOK3 protein is increased in MDA-MB-231 cells treated with 0.5 mM DMOG for 24 h. Cells were transduced with pTRIPZ lentivirus expressing shRIOK3 in a doxycycline-inducible manner. Indicated samples were treated with 1 μg/mL doxycycline (Dox) for 24 h prior to and during treatment with DMOG.

Figure S4: (A) The relocalisation of RIOK3 that occurs during hypoxia is dependent on HIF-1α. MDA-MB-231 cells were transfected with siCon or siHIF-1α, exposed to normoxia or hypoxia for 24 h and then stained for RIOK3. RIOK3 aggregates are indicated by arrowheads. (B) MDA-MB-231 cells transduced with shCon are smaller and more rounded than the elongated phenotype observed for shRIOK3 cells.

Fig S5: RIOK3 knockdown does not effect cell proliferation. (A) Efficiency of RIOK3 mRNA knockdown in MDA-MB-231 cells transduced with lentivirus expressing doxycycline-inducible shRNA measured by RT-qPCR (n = 2). (B) Efficiency of RIOK3 protein knockdown in MDA-MB-231 cells transduced with lentivirus expressing doxycycline-inducible shRNA measured by immunoblot. (C) Effect of doxycycline-inducible shRIOK3 expression on proliferation of MDA-MB-231 cells in 2D measured by CyQuant (n = 2). (D) Invasion of MDA-MB-231 cells transduced with lentivirus expressing doxycycline-inducible shRNA in normoxia or hypoxia.

Treatment of pTRIPZ shRIOK3 cells with 1 μg/mL doxycycline (Dox) reduced the amount of invasion through matrigel in both normoxia and hypoxia. Treatment of pTRIPZ shNS (control) cells with 1 μg/mL doxycycline had no effect on cell invasiveness.

Fig S6: RIOK3 promotes 2D cell migration and 3D invasion in SK-OV-3 cells. (A) Immunoblot demonstrating RIOK3 expression in SK-OV-3 cells transfected with siCon or siRIOK3. (B) Modified scratch wound assay shows the % wound area closed at 7 h was decreased in normoxia and hypoxia following transfection of SK-OV-3 cells with siRIOK3 (mean ± SEM, n = 3). (C) Representative modified scratch wound assay images of SK-OV-3 cells transfected with siCon or siRIOK3 in normoxia/hypoxia at time 0 and after 7 h. (D) Representative 3D invasion assay micrographs for SK-OV-3 cells transfected with siCon or siRIOK3 after 24 h invasion in normoxia/hypoxia.

Fig S7: Analogue sensitive RIOK3 does not produce novel thiophosphorylations when incubated with $N^6$-Benzyladenosine-5'-O-3-thiotriphosphate (A) amino acid sequence alignment of Rio1 from *Archaeoglobus fulgidus* DSM 4304 (AfRio1) and human RIOK3 (HsRIO3). The gatekeeper residues M147 (AfRio1) and M359 (HsRIO3) are highlighted in red. (B) Analogue sensitive kinase assay demonstrating thiophosphate modification in lysates of HEK-293 cells expressing either wild-type RIOK3 (WT), RIOK3 mutant M359G or untransduced (Unt) control cells. Untreated whole cell lysates contain higher levels of RIOK3 than the lysates from permeabilised cells used for the analogue sensitive kinase assay, suggesting that

much of the RIOK3 has escaped from the cells during permeabilisation. No novel thiophosphorylations were detected in cells expressing RIOK3 with a gatekeeper mutation (M359G).

Figure S8: Fluorescence recovery after photobleaching (FRAP) of GFP-RIOK3 in MDA-MB-231 cells. (A) After an initial image was captured a photobleach was done indicated by the dashed blue line. The cytoplasmic area of photobleach is indicated by a dashed red square in the first image. Serial images were captured every 24 seconds. Phase contrast images are presented below the fluorescent image. (B) A second photobleach was carried out in the same area of the cytoplasm. (C) Magnified region of (A) indicated by dashed yellow line showing cytoplasmic structure that excludes GFP-RIOK3 (red arrowhead). (D) Magnified region of (B) indicated by dashed yellow line showing cytoplasmic structure that is enriched for GFP-RIOK3 (yellow arrowhead). Scale bar = 10 μm.

Video S1: Timelapse video of MDA-MB-231 migration. Images of siCon cells (left) and siRIOK3 cells (right) were captured every 5 min for a total of 5 h. Videos were generated at 6 frames/second, total 10 seconds.

Fig S1

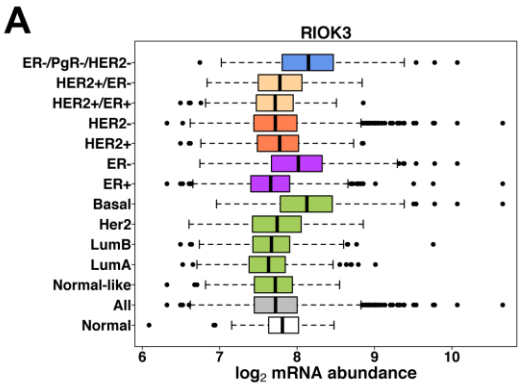


B

| | RIOK3 | | | | |
|---|---|---|---|---|---|
| PAM50 subtype | Log2 fold change | lwr | upr | P value | signif |
| Her2-Basal | -0.410 | -0.507 | -0.313 | 0.00E+00 | *** |
| LumA-Basal | -0.530 | -0.606 | -0.454 | 0.00E+00 | *** |
| LumB-Basal | -0.473 | -0.554 | -0.392 | 0.00E+00 | *** |
| Normal-Basal | -0.358 | -0.473 | -0.244 | 0.00E+00 | *** |
| Normal-like-Basal | -0.452 | -0.554 | -0.350 | 0.00E+00 | *** |
| LumA-Her2 | -0.120 | -0.205 | -0.034 | 9.25E-04 | *** |
| LumB-Her2 | -0.063 | -0.153 | 0.027 | 3.50E-01 | |
| Normal-Her2 | 0.052 | -0.069 | 0.172 | 8.28E-01 | |
| Normal-like-Her2 | -0.042 | -0.151 | 0.068 | 8.86E-01 | |
| LumB-LumA | 0.057 | -0.010 | 0.124 | 1.48E-01 | |
| Normal-LumA | 0.172 | 0.067 | 0.276 | 4.52E-05 | *** |
| Normal-like-LumA | 0.078 | -0.013 | 0.169 | 1.42E-01 | |
| Normal-LumB | 0.115 | 0.006 | 0.223 | 3.17E-02 | * |
| Normal-like-LumB | 0.021 | -0.075 | 0.117 | 9.89E-01 | |
| Normal-like-Normal | -0.093 | -0.218 | 0.032 | 2.71E-01 | |

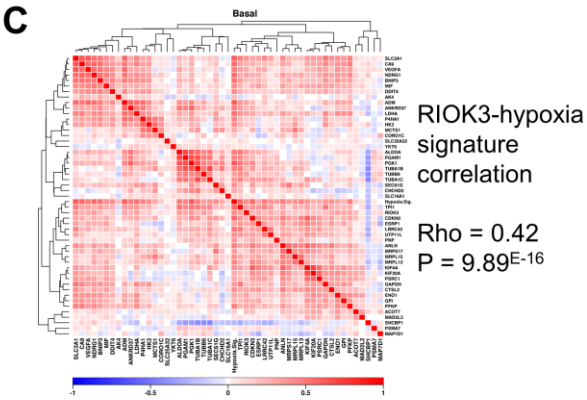


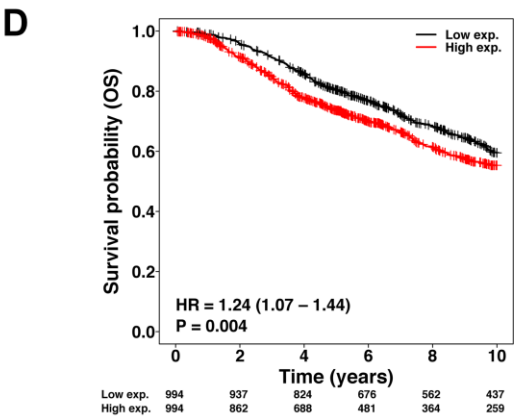

Fig S2

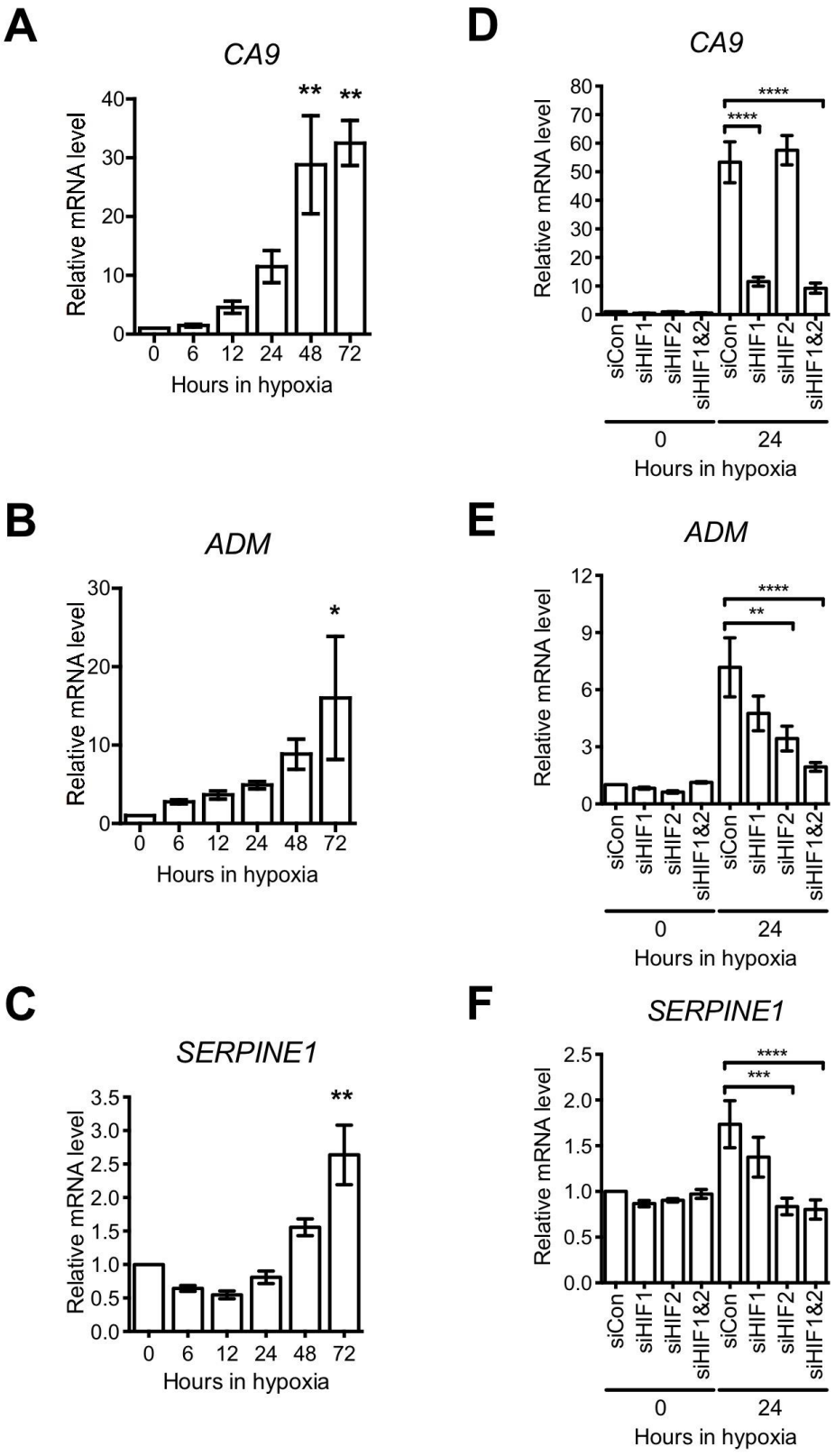
A
CA9
Relative mRNA level
Hours in hypoxia
B
ADM
Relative mRNA level
Hours in hypoxia
C
SERPINE1
Relative mRNA level
Hours in hypoxia
D
CA9
Relative mRNA level
siCon
siHIF1
siHIF2
siHIF1&2
Hours in hypoxia
E
ADM
Relative mRNA level
Hours in hypoxia
F
SERPINE1
Relative mRNA level
Hours in hypoxia

Fig S3

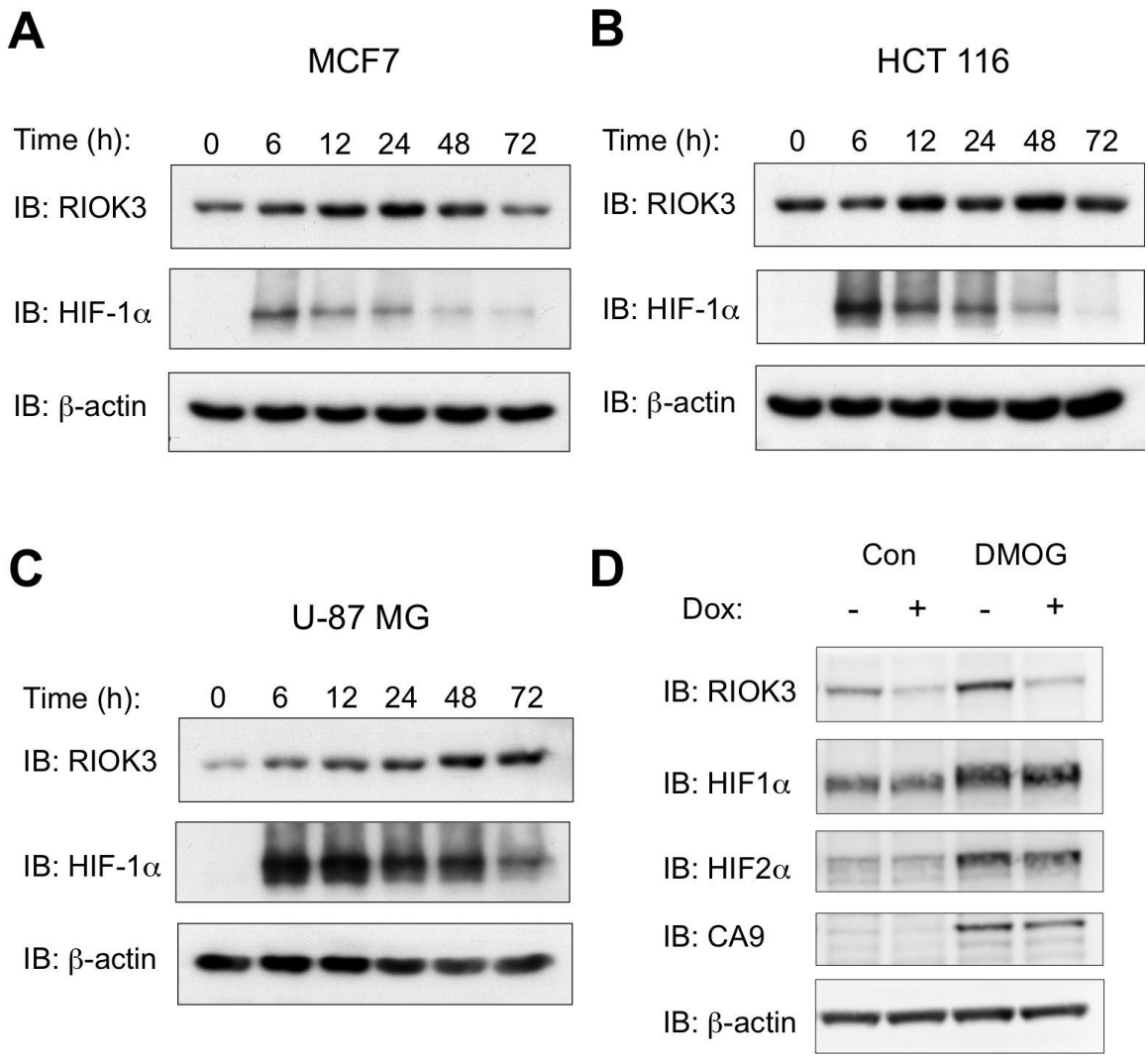
A
MCF7
Time (h): 0 6 12 24 48 72
IB: RIOK3
IB: HIF-1α
IB: β-actin
B
HCT 116
Time (h): 0 6 12 24 48 72
IB: RIOK3
IB: HIF-1α
IB: β-actin
C
U-87 MG
Time (h): 0 6 12 24 48 72
IB: RIOK3
IB: HIF-1α
IB: β-actin
D
Con DMOG
Dox: - + - +
IB: RIOK3
IB: HIF1α
IB: HIF2α
IB: CA9
IB: β-actin

Fig S4

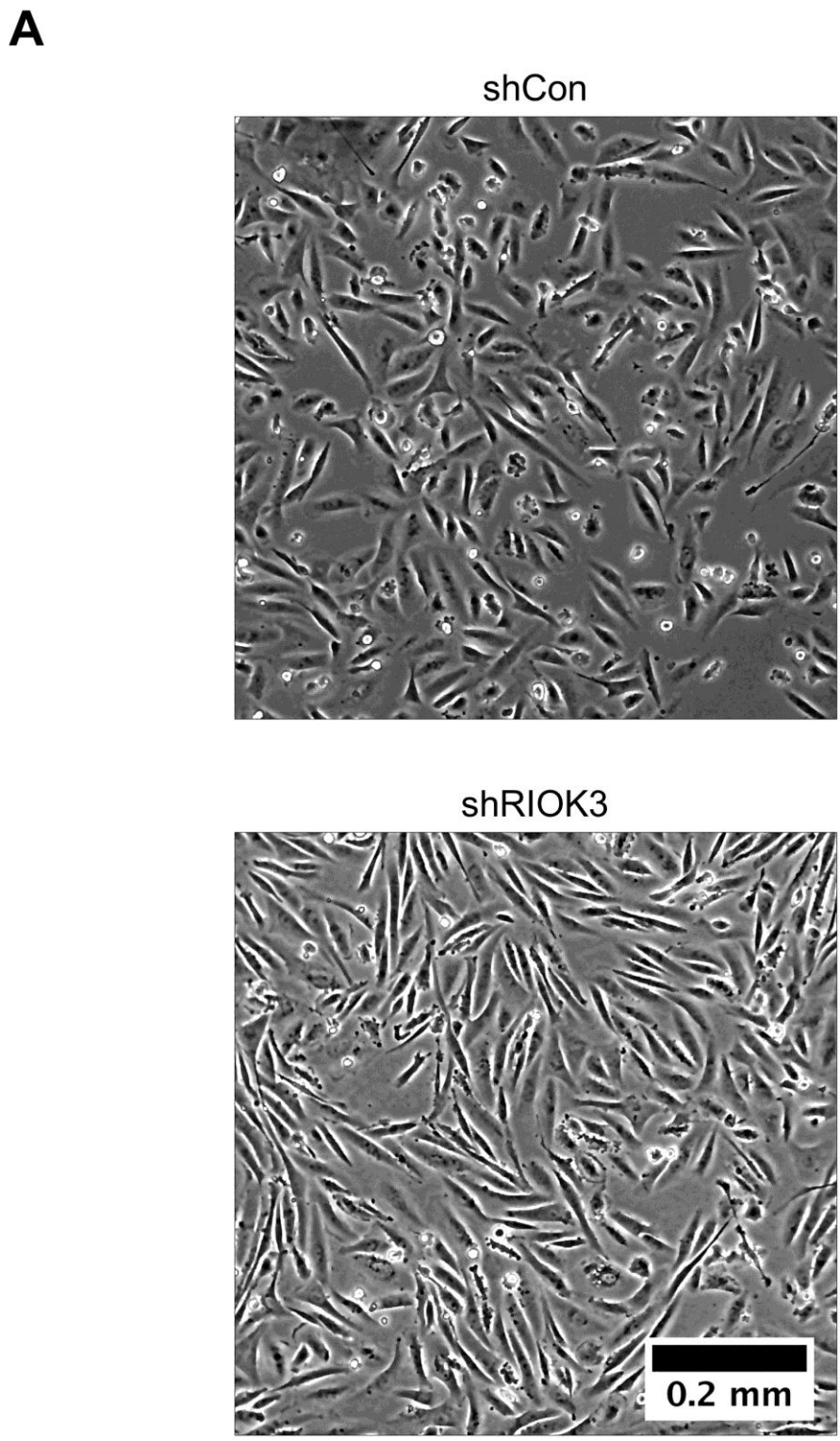

Fig S5

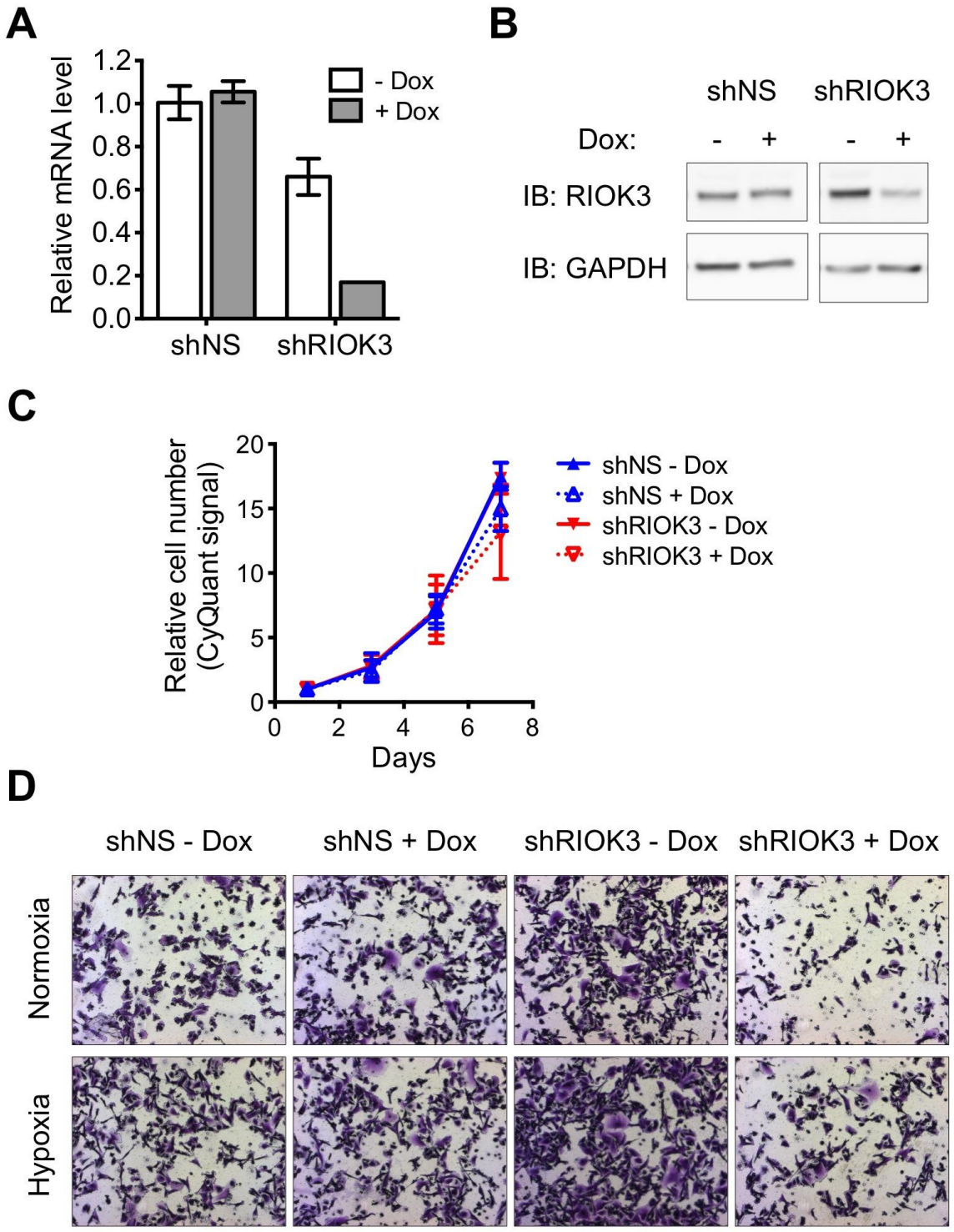
A
Relative mRNA level
1.2
1.0
0.8
0.6
0.4
0.2
0.0
- Dox
+ Dox
shNS
shRIOK3
B
shNS
shRIOK3
Dox:
- + - +
IB: RIOK3
IB: GAPDH
C
Relative cell number (CyQuant signal)
20
15
10
5
0
0 2 4 6 8
Days
shNS - Dox
shNS + Dox
shRIOK3 - Dox
shRIOK3 + Dox
D
shNS - Dox
shNS + Dox
shRIOK3 - Dox
shRIOK3 + Dox
Normoxia
Hypoxia

Fig S6

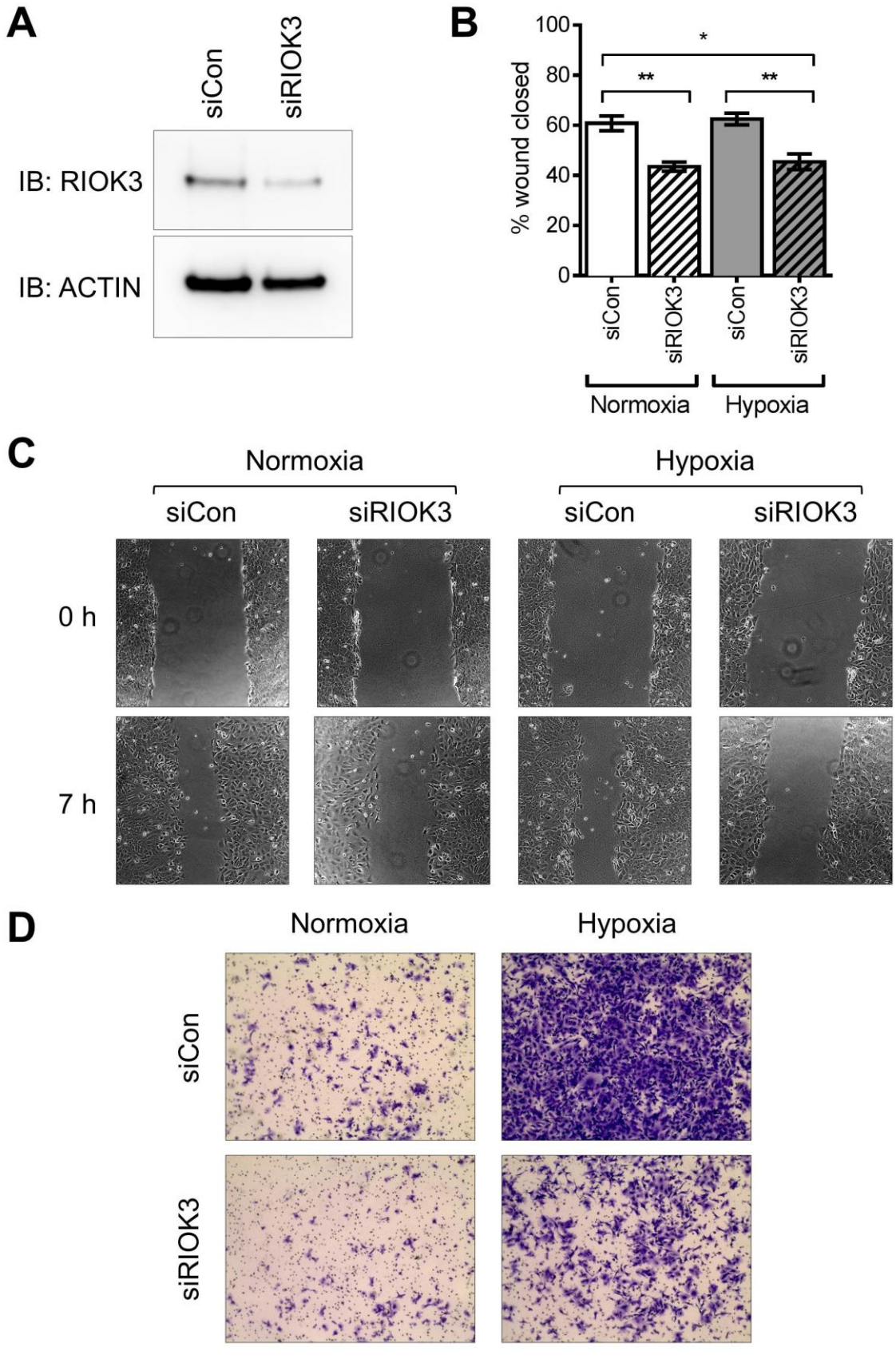
A
siCon
siRIOK3
IB: RIOK3
IB: ACTIN
B
% wound closed
100
80
60
40
20
0
*
**
**
siCon
siRIOK3
siCon
siRIOK3
Normoxia
Hypoxia
C
Normoxia
Hypoxia
siCon
siRIOK3
siCon
siRIOK3
0 h
7 h
D
Normoxia
Hypoxia
siCon
siRIOK3

Fig S7

**A**

```
AfRio1 15   RIKEKDGEERKIYAEVLDGRTLKTLYKLSAKGYITAMGGVISTGKEANVFYADGVF----  70
            R+ EK  +E     + +D +T   +YK+   G +  + G ISTGKE+ VF+A G
HsRIO3 219  RLHEK--KEHSTAEKAVDPKTRLLMYKMVNSGMLETITGCISTGKESVVFHAYGGSMEDE  276

AfRio1 71   --DGK--PVAMAVKIYRIETSEFDKMDEYLYGDERFDMR--RISPKEKVFIWTEKEFRNL  124
              D K  P   A+K+++   +EF   D+Y+  D RF  R  +++P++ + +W EKE  NL
HsRIO3 277  KEDSKVIPTECAIKVFKTTLNEFKNRDKYIKDDFRFKDRFSKLNPRKIIRMWAEKEMHNL  336

AfRio1 125  ERAKEAGVSVPQPYTYMKNVLLMEFIGEDELPAPTLVELGRELKELDVEGIFNDVVENVK  184
             R + AG+  P      K++L+M FIG D++PAP L E+  +L   +++  +   + ++
HsRIO3 337  ARMQRAGIPCPTVVLLKKHILVMSFIGHDQVPAPKLKEV--KLNSEEMKEAYYQTLHLMR  394

AfRio1 185  RLYQEAELVHADLSEYNIMY-IDKVYFIDMGQAVTLRHPMAESYLERDVRNIIRFFSKYG  243
            +LY E  LVHADLSEYN+++   KV+ ID+ Q+V   HP    +L RD RN+ +FF K G
HsRIO3 395  QLYHECTLVHADLSEYNMLWHAGKVWLIDVSQSVEPTHPHGLEFLFRDCRNVSQFFQKGG  454

AfRio1 244  VKADFEE  250
            VK    E
HsRIO3 455  VKEALSE  461
```

**B**

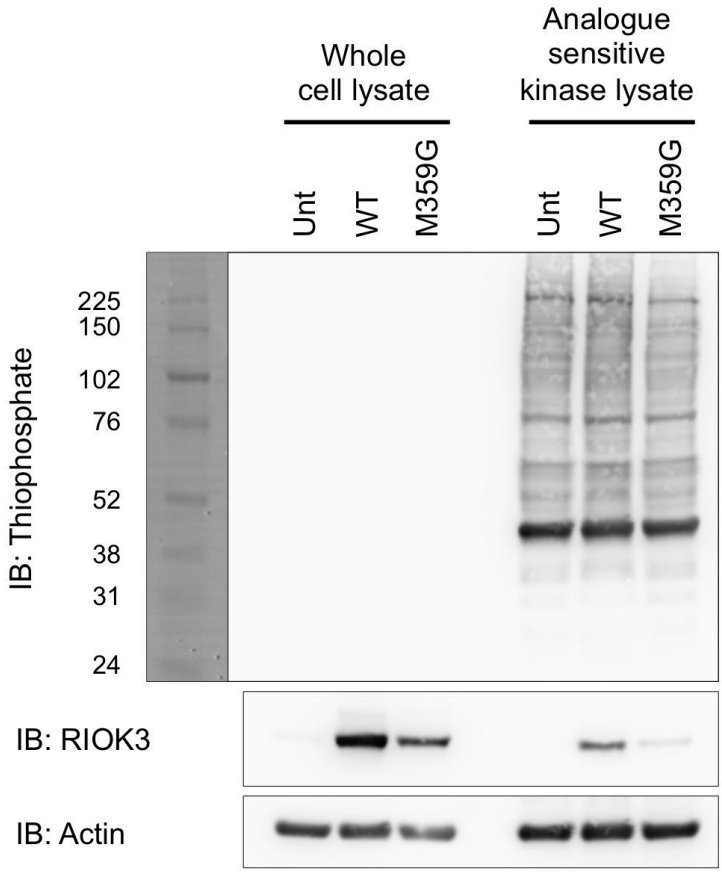

Fig S8

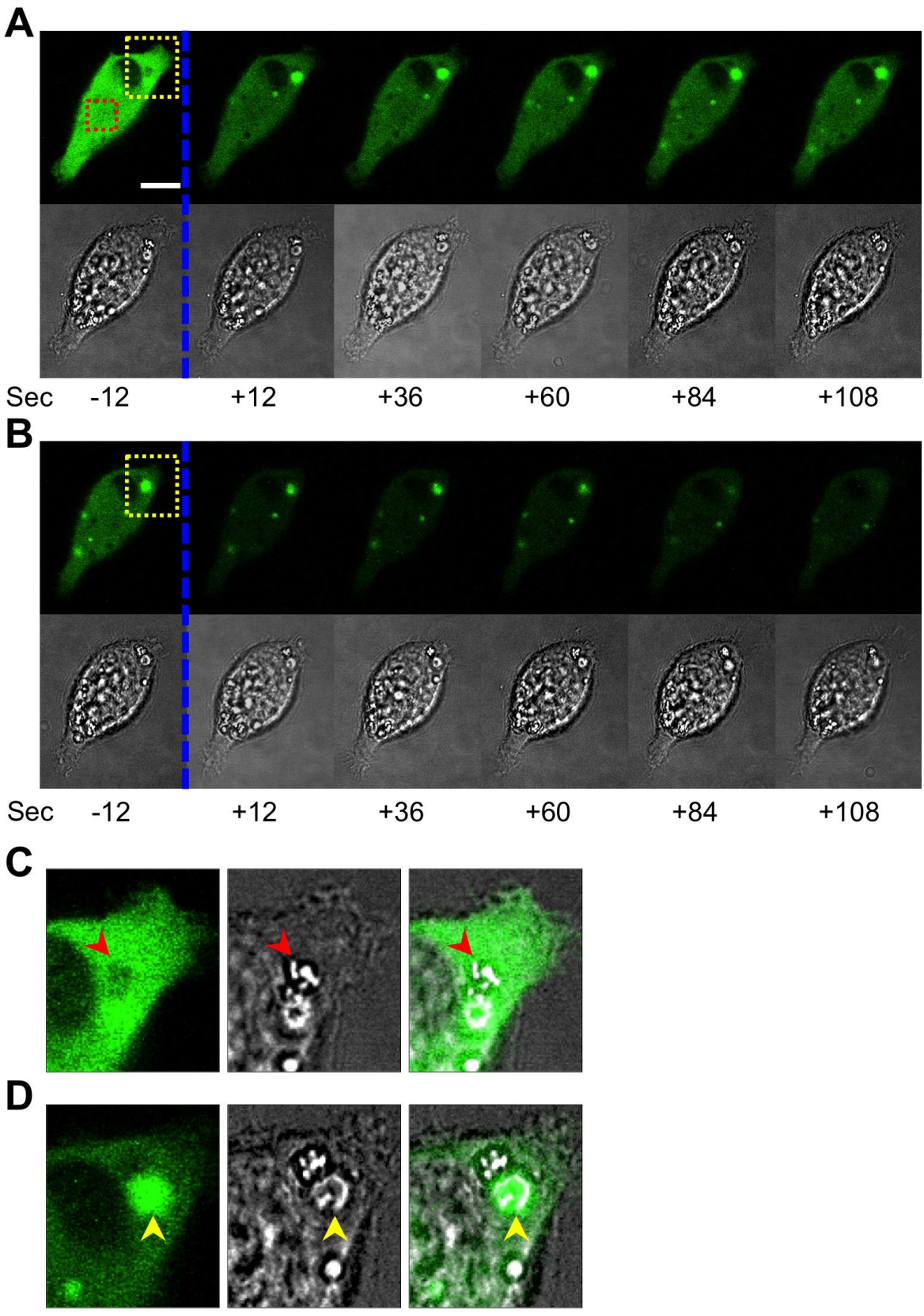

Video S1 (Still image)